

# Compact 80 W, 1 MHz Femtosecond Chirped Pulse Amplification Laser System Based on a Yb-Doped Fiber and a Yb:YAG Thin Rod

Yan Xu , Zhigang Peng , Yuhang Shi , Beibei Wang, Zhaochen Cheng, and Pu Wang

**Abstract**—We present a hybrid chirped pulse amplification (CPA) laser system based on Yb-doped fiber and Yb:YAG thin rod. The laser system demonstrates a novel approach to generate high average power up to the 100-W level by using a Yb:YAG thin rod without pump guiding at room temperature. A Yb-doped all-fiber laser with an output power of 7 W and a repetition rate of 1 MHz is amplified to an output power of 126.2 W in simple and compact two-stage amplifiers consisting of a single fiber crystal (SCF) and a Yb:YAG thin rod. To the best of our knowledge, this is the highest output power of Yb:YAG thin-rod amplifier with good beam quality obtained without pump guiding at room temperature. After using a thin-film polarizer (TFP) to remove the thermal depolarization, a linearly polarized ultrashort pulse laser with an average power of 115.2 W is obtained. An output power of 80.6 W with a pulse width of 580 fs is achieved after pulse compression. The central pulse contains 84.1% of the total pulse energy, corresponding to a pulse peak power of 116.9 MW.

**Index Terms**—Chirped pulse amplification, femtosecond laser, hybrid amplification, Yb:YAG thin rod.

## I. INTRODUCTION

THERE is widespread demand for ultrashort-pulse lasers with high average power and high peak power for industrial and scientific applications, such as laser manufacturing processes, high harmonic generation, and nonlinear frequency conversion [1]–[6].

Yb-doped fiber lasers present the advantages of high optical-to-optical efficiency, good beam quality, and maintenance-free operation. However, for amplifying ultrashort pulses, the small core diameter of the fiber restricts the peak power and pulse energy due to the nonlinear effects caused by high power intensities and long interaction length in the fiber, such as self-phase modulation (SPM) and stimulated Raman scattering

(SRS). Increasing the mode field area of the fiber amplifier or using chirped-pulse amplification (CPA) technology is a viable method for lowering power intensities. Nevertheless, due to the limitation of the self-focusing effect, the maximum peak power of silica fiber is less than 4 MW [7]–[9].

Yb:YAG crystals, benefiting from low nonlinear effects, excellent thermo-optical properties, and high peak power tolerance, combined with a Yb-doped all-fiber front end, can generate compact and stable ultrashort pulsed laser sources with high average power and high peak power. However, the crystals require effective heat dissipation at high power pumping. Cryogenic Yb:YAG crystals have excellent thermo-optic properties and emission cross-sections, but the narrowed emission spectrum is not supportive of subpicosecond pulses [10], [11]. Thin disk and InnoSlab amplifiers provide efficient thermal management, but require complex pumping schemes that are inevitably expensive and reduce system stability [12], [13].

Single crystal fibers (SCFs) are thin rods usually with a diameter from 400  $\mu\text{m}$  to 1.5 mm and a length of a few centimeters that are used as a waveguide for multimode pump light and as a bulk crystal for signal [14], [15]. They greatly improve pump absorption and optical-to-optical conversion efficiency compared to bulk crystals, and over the last decade, they have shown good potential for high power amplification with a simple and compact configuration. In 2015, Markovic *et al.* obtained an average power of 160 W with a relatively low pulse energy of 1.9  $\mu\text{J}$  at a repetition rate of 83.4 MHz based on two-stage Yb:YAG SCF amplifiers [16]. Due to the small aperture of the SCF, there is a risk of damage to the antireflective (AR) coating of the end face when delivering high peak power pulses. Therefore, divided pulse amplification (DPA) technology or chirped pulse amplification (CPA) technology is required to achieve ultrashort pulses with high peak power. In 2016, Lesparre *et al.* obtained an average power of 55 W with a repetition rate of 12.5 kHz with DPA technology using two Yb:YAG SCF amplifiers [17]. In 2020, Wang *et al.* reported a CPA system consisting of an all-fiber front end, a direct water-cooled Yb:YAG rod amplifier and two-stage SCF amplifiers; an output power of 96 W was obtained before compression [18], [19]. In 2021, Yang *et al.* obtained an output power of 130 W using three-stage Yb:YAG SCF amplifiers with CPA technology. The main amplifier is a Taranis module integrating a 30 mm long Yb:YAG SCF with 1 at.% doping rate. When the pump power of the Taranis module was 262 W, the beam quality is degraded from  $M_{x,y}^2 = 1.09 \times 1.23$  in the

Manuscript received January 28, 2022; revised February 22, 2022; accepted March 4, 2022. Date of publication March 8, 2022; date of current version March 17, 2022. This work was supported in part by the National Key R&D Program of China under Grant 2017YFB0405201 and in part by the National Natural Science Foundation of China under Grant 62035002. (Corresponding authors: Zhigang Peng; Pu Wang.)

The authors are with the Beijing Engineering Research Center of Laser Technology, Beijing University of Technology, Beijing 100124, China, with the Key Laboratory of Trans-Scale Laser Manufacturing Technology, Beijing University of Technology, Beijing 100124, China, and also with the Institute of Laser Engineering, Faculty of Materials and Manufacturing, Beijing University of Technology, Beijing 100124, China (e-mail: xuyanemail@yeah.net; pzg@bjut.edu.cn; yhshi@emails.bjut.edu.cn; wangb@emails.bjut.edu.cn; chengzhaochen@bjut.edu.cn; wangpuemail@bjut.edu.cn).

Digital Object Identifier 10.1109/JPHOT.2022.3157668

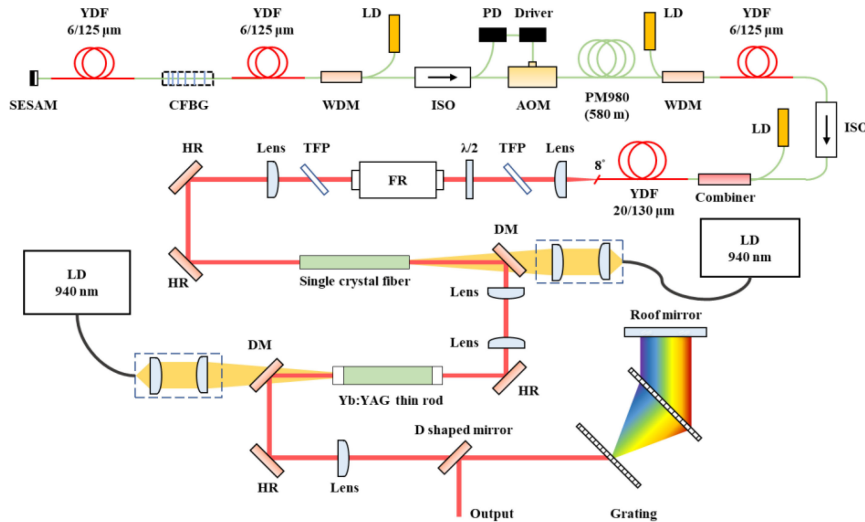


Fig. 1. Schematic of hybrid Yb-doped fiber and Yb:YAG thin-rod CPA system. LD, laser diode; WDM: filter wavelength division multiplexer; YDF, Yb-doped fiber; LD, laser diode; PD, photodetector; AOM, acoustic optical modulator; ISO, isolator; TFP, thin-film polarizer; FR, Faraday rotator; HR, high reflection mirror; DM, dichroic mirror.

second stage to  $M_{x,y}^2 = 1.63 \times 1.90$  [20]. Although SCFs have been successfully used for high power amplification, the process of manufacturing SCF modules is relatively complicated, and the cost is high.

Benefiting from the brightness improvement provided by the pump laser diode (LD), the Yb:YAG thin rod has also obtained high average power at room temperature in the last few years. In addition, Yb:YAG thin rods are much less expensive than Yb:YAG SCFs due to their simple preparation process. In 2017, Rodin *et al.* used a 2 at.% doped Yb:YAG thin-rod amplifier with dimensions of 2 mm  $\times$  2 mm  $\times$  20 mm to amplify a 500 mW seed beam to 47.3 W at 500 kHz [21]. In 2019, Chu *et al.* demonstrated a master oscillator power amplifier (MOPA) laser system with a Yb:KGW oscillator and two Yb:YAG amplifiers to directly amplify a signal with a pulse width of 1.87 ps and repetition rate of 1 MHz; an output power of 8.2 W was obtained with a pulse width of 4.66 ps [22]. In 2020, Veselis used a 3.6 at.% doped Yb:YAG rod with a length of 12 mm to generate an average power of 40 W at 1 MHz [23]. However, highly doped short rods led to deleterious thermal effects that were not conducive to high power amplification. Moreover, we reported a hybrid Yb-doped fiber and three-stage 1 at.% doped Yb:YAG thin rod MOPA system, and an average power of 100 W with a repetition rate of 20 MHz was obtained. The beam quality factor was 4 because the cooling method led to poor heat dissipation and temperature uniformity at high-power pumping [24].

From the perspective of system complexity, to obtain output power at the 100-W level using the current Yb:YAG SCF and thin rod usually requires at least three-stage amplifiers, which is not conducive to building laser systems.

In this paper, our objective is to demonstrate the high power amplification capability of Yb:YAG thin rods without pump guiding at room temperature and reduce the complexity and cost of the 100 W-level Yb:YAG laser system. We present a hybrid CPA laser system consisting of an all-fiber front end,

a Yb:YAG SCF pre-amplifier, and a Yb:YAG thin-rod main amplifier. An output power of 126.2 W with a beam quality of  $M_{x,y}^2 = 1.83 \times 1.61$  is obtained through a compact two-stage Yb:YAG amplifier configuration, effectively reducing the complexity of the system. This result also demonstrates the ability of Yb:YAG thin rods without pump guiding to achieve high average power comparable to that of the Yb:YAG SCF amplifier at room temperature with good beam quality. To the best of our knowledge, this paper reports the highest output power of a Yb:YAG thin rod (without pump guiding) by using compact two-stage amplifiers with CPA technology at 1 MHz. After using a thin-film polarizer (TFP) to remove the thermal depolarization, a 115.2 W linearly polarized ultrashort-pulse laser is obtained, with a center wavelength of 1029.8 nm and a pulse width of 242.1 ps. Following compression by a pair of diffraction gratings, a pulse width of 580 fs with an average power of 80.6 W is obtained.

## II. EXPERIMENTAL SETUP

A schematic of the hybrid Yb-doped fiber and Yb:YAG thin-rod laser system is shown in Fig. 1. The seed consists of a polarization-maintaining (PM) passive mode-locked fiber oscillator with a linear cavity and a Yb-doped fiber pre-amplifier. The oscillator operates in the dispersion-management regime through a chirped fiber Bragg grating (CFBG) with an anomalous dispersion  $\beta_2 = -0.1139$  ps<sup>2</sup>. A piece of Yb-doped PM fiber (Nufern, PM-YSF-HI-6/125) with a length of 1 m and an absorption coefficient of 250 dB/m at 976 nm is used as the gain medium. A semiconductor saturable absorber mirror (SESAM) with a modulation depth of 30% is used in the cavity to establish self-start mode locking. The pre-amplifier with a 0.5 m long Yb-doped PM fiber is pumped by the 976 nm LD which is also a pump source for the oscillator. An acoustic optical modulator (AOM) is used to reduce the repetition rate of the seed.

The pulse is then stretched through a 580 m long single mode fiber. The stretched pulse is amplified by two-stage Yb-doped PM fiber amplifiers. All the amplifiers were forward pumped. After an isolator, a pump-signal combiner is used to deliver the pump light into the main amplifier of the all-fiber front end, which is a 2 m long double-clad 20/130  $\mu\text{m}$  Yb-doped PM fiber (Nufern, PLMA-YDF-20/130-VIII) with a cladding absorption coefficient of 10.2 dB/m at 976 nm. The reflection of light from the fiber end face is eliminated by cutting an 8° angle at the fiber output.

In the first Yb:YAG pre-amplifier, the gain medium is a 1 at. % doped Yb:YAG SCF (Taranis module, Fibercryst Inc.) with dimensions of  $\Phi 1 \text{ mm} \times 30 \text{ mm}$ . The seed beam is collimated to a 420  $\mu\text{m}$  diameter spot inside the SCF. The pump source is a 200 W fiber-coupled LD (BWT Inc.) operating at 940 nm. The diameter of the fiber is 135  $\mu\text{m}$  with a numerical aperture (NA) of 0.22. The pump beam is imaged into the SCF with a diameter of 408  $\mu\text{m}$  using two plano-convex lenses with focal lengths of 50 and 150 mm. After amplification, the laser beam from the SCF pre-amplifier is injected into the main amplifier. In the main amplifier, the gain medium is a 2 mm diameter, 50 mm long, 1 at. % doped Yb:YAG thin rod with an unpolished barrel surface, which has 5 mm long undoped end caps at both ends. The crystal is mounted in a water-cooled copper microchannel heat sink with a temperature of 16°C and is clamped by contact with two semicylindrical copper grooves filled with thermal grease. Three 150 W fiber-coupled LDs at a center wavelength of 940 nm are combined by a 3×1 combiner for the Yb:YAG thin-rod amplifier. The pigtail diameter of the combiner is 200  $\mu\text{m}$  with an NA of 0.22. The pump beam is imaged into the crystal with a diameter of 604  $\mu\text{m}$ . The signal is then injected into the Yb:YAG thin-rod main amplifier with slight divergence. The spot diameter of the signal measured at the pump waist location is 690  $\mu\text{m}$ . The amplified laser beam is then compressed by a pair of transmission gratings (LightSmyth.T-1600-1030s-130X20-94) with a grooved grating of 1600 line/mm.

### III. EXPERIMENTAL RESULTS AND DISCUSSIONS

In the all-fiber front end, the seed output had an average power of 64.6 mW with a spectral width of 26.1 nm. The AOM was used to reduce the repetition rate from 52.9 MHz to 1 MHz. After stretching, the pulse was amplified to 16.7 mW by the first fiber amplifier. The pulse trains of the seed and the first fiber amplifier were measured in real time by a 25 GHz real-time oscilloscope with a 15 GHz InGaAs photodetector, as shown in Fig. 2. Then, the signal was amplified to an average power of 11.0 W by a double-clad gain fiber amplifier, as shown in Fig. 3.

The SCF pre-amplifier obtained an average power of 42.8 W through single-pass amplification at a pump power of 182 W when the signal power was 7 W. Fig. 4 shows the output power of the SCF amplifier as a function of pump power. As the pump power increased, the amplification efficiency of the SCF pre-amplifier decreased. We believe that the reason is the temperature increase of the SCF. Notably, we employed a TFP to remove the thermal depolarization power of 1.0 W, so the signal power delivery to the next stage was 41.8 W.

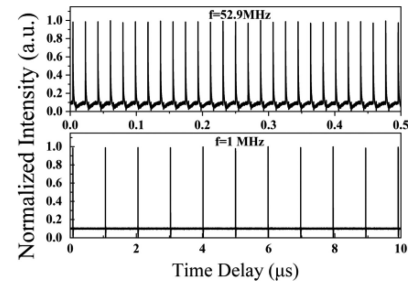


Fig. 2. Temporal pulse trains of the seed and all-fiber front end.

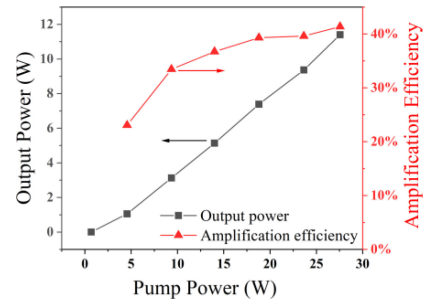


Fig. 3. Output power versus pump power of the 20/130  $\mu\text{m}$  double-clad gain fiber amplifier.

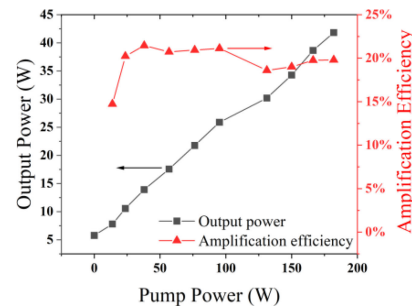


Fig. 4. Output power versus pump power of the Yb:YAG SCF pre-amplifier.

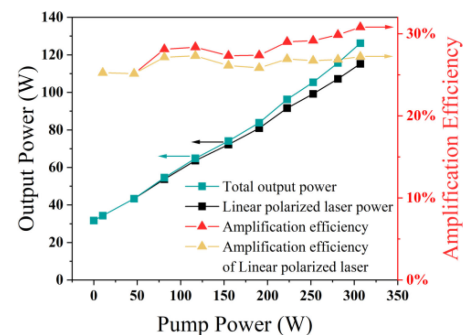


Fig. 5. Output power versus pump power of the Yb:YAG thin-rod amplifier.

The Yb:YAG thin rod amplified the signal from 41.8 W to 126.2 W at a pump power of 307.0 W, which was higher than the recommended maximum pump power of 200 W for the SCF module. After removing the thermal depolarization, an output power of 115.2 W with linear polarization was obtained. The



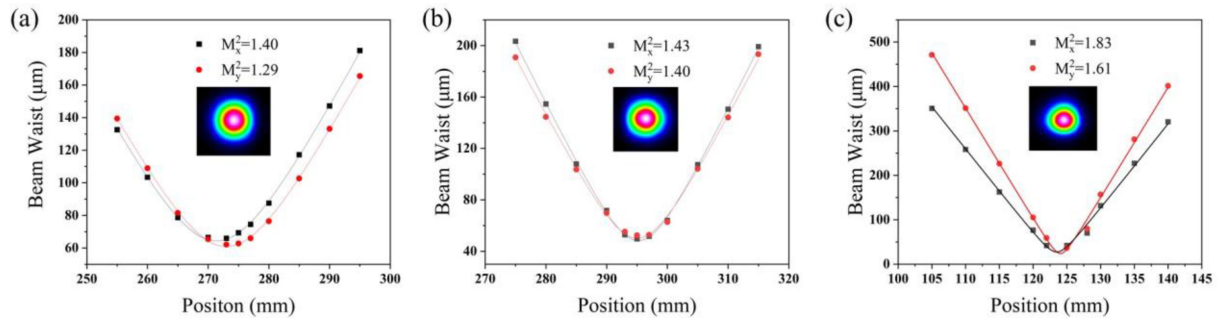


Fig. 6. Output beam profiles and beam quality of (a) All-fiber front end, (b) Yb:YAG SCF pre-amplifier, and (c) Yb:YAG thin-rod main amplifier.

relationship between the pump power and output power is shown in Fig. 5. The beam quality factors were measured by a scanning slit beam profiler. The values of  $M_x^2$  and  $M_y^2$  degraded from 1.40 and 1.29 at the all-fiber front end to 1.83 and 1.61 for the Yb:YAG thin-rod amplifier along the vertical direction and horizontal direction, respectively, as shown in Fig. 6. We estimate that the desired beam quality is not achieved because the end face of the fiber output exhibits distortion when the fiber cleaver cuts an angle of 8 degrees, causing deterioration of the beam quality.

Thermal grease, as a thermal interface material, has better thermal contact due to its good fluidity and does not stress the crystal. The microchannel heat sink has good heat dissipation efficiency and can evenly dissipate heat on a large surface. In the experiment, the Yb:YAG thin rod was placed in the middle of two microchannel heat sinks, and the length direction of the thin rod was perpendicular to the direction of the water flow in the microchannel. The cooling water only passes near the Yb:YAG thin rod once, which will not further affect the temperature of Yb:YAG thin rod. Therefore, thermal grease and microchannel heat sinks can provide efficient thermal management for thin rods due to their excellent heat dissipation and uniform temperature distribution [25]–[27].

Refractive index changes in solid-state gain media under high-power pumping are caused by thermal effects and an electron (population) lens, which can affect the beam quality of lasers. In the Yb:YAG crystal, the electron lens is small under the continuous-wave pumping condition. Moreover, under lasing conditions, the reduction in the excited state population causes a decrease in the electron lens, so the electron lens can be negligible. We only need to consider the degradation of the beam quality due to thermal effects [28], [29]. In this work, benefiting from the thermal management of the microchannel heat sink, the beam quality degradation was not severe when the pump power exceeded 300 W. By using a seed laser with good beam quality, the beam quality of the Yb:YAG main amplifier can be improved, as shown in our previous work [30]. We believe that the increase in thermal depolarization power indicates that the temperature distribution of the thin rod changes with high pump power, because thermal depolarization is positively correlated with thermal loading [31], [32]. As shown in the inset of Fig. 5, the amplified beam profile was elliptical, because the thermal conductivity of thermal grease ( $6 \text{ W m}^{-1} \text{ K}^{-1}$ ) at the heat

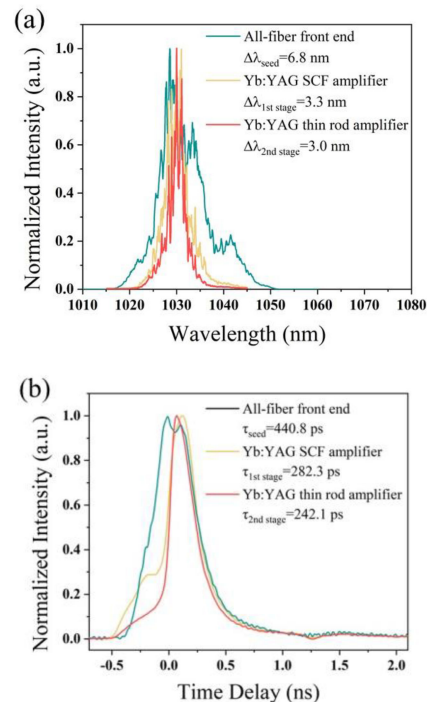


Fig. 7. (a) Spectrum evolution and (b) Pulse width of the all-fiber front end and two-stage Yb:YAG amplifiers.

sink junction was lower than that of copper ( $400 \text{ W m}^{-1} \text{ K}^{-1}$ ), resulting in uneven heat dissipation in the horizontal and vertical directions. The amplification efficiency remained flat at approximately 30%, indicating that the heat dissipation of the microchannel heat sink was still effective, as shown in Fig. 6 (red and orange curves).

A laser spectrometer (Yokogawa, AQ6370D) with a resolution bandwidth of 0.02 nm was employed to record the output spectrum. Fig. 7(a) shows the spectral evolution of the all-fiber front end and two-stage Yb:YAG amplifiers. High gain leads to a strong gain narrowing effect. The width of the spectrum amplified by SCF is narrowed from 6.8 nm to 3.3 nm. The spectrum width further narrowed to 3.0 nm at the Yb:YAG thin-rod amplifier. The pulse widths measured by the 25 GHz real-time oscilloscope were 440.8 ps, 282.3 ps, and 242.1 ps for the all-fiber front end, SCF amplifier, and Yb:YAG thin-rod

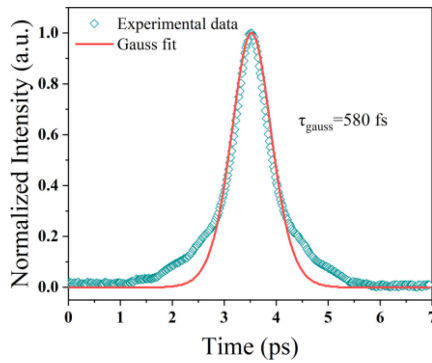


Fig. 8. Measured intensity autocorrelation traces of the compressed pulses.

amplifier, respectively, as shown in Fig. 7(b). The narrowing of the chirped pulse duration was caused by the mapping from the frequency domain to the time domain, as the stretched pulse had a positive chirp, resulting in the pulse profile related to the spectral profile [33]. The temporal performance of the photodetector is specified by the rise time. The temporal trace will be smoother than the spectral trace and will exhibit certain differences at the edges of the trace.

The pulse was compressed by a pair of transmission gratings. A compressed power of 80.6 W was achieved, with a corresponding compression efficiency of 70.0%, as shown in Fig. 8. The pulse duration of 580 fs was measured by the autocorrelator (APE GmbH). A peak power of 116.9 MW is obtained considering the 84.1% of the total energy in the central pulse. Because of the third-order dispersion of the stretching fiber, the compression pulse duration was wider than the Fourier transform-limited pulse duration of 521 fs. Narrower pulse widths may be achieved by stretching pulses using CFBGs with low third-order dispersion, which will be the focus of our future research.

#### IV. CONCLUSION

In conclusion, we demonstrated a compact hybrid CPA system that is based on a Yb-doped all-fiber front end and two-stage Yb:YAG amplifiers with an output power of 126.2 W at a repetition rate of 1 MHz. To the best of our knowledge, this is the highest output power of a Yb:YAG thin rod without pump guiding that has been reported at room temperature. Beam quality factors of 1.83 and 1.61 were measured along the vertical and horizontal directions, respectively. The output power of 115.2 W with linear polarization was obtained, after removing thermal depolarization. A pulse duration of 580 fs was achieved after compression with an average power of 80.6 W and a peak power of 116.9 MW after disregarding the energy in the pulse side-wings. The experimental results showed that a laser amplifier system employing a Yb:YAG thin rod without pump guiding can provide a high average power at room temperature for low cost. By optimizing the dimensions and doping of the crystal and using zero-phonon line pumping, the amplified average power can be further increased. This system shows promise as a laser source for industrial manufacturing and scientific research.

#### REFERENCES

- [1] S. Lei *et al.*, "Ultrafast laser applications in manufacturing processes: A State-of-the-art review," *J. Manuf. Sci. Eng.*, vol. 142, no. 3, Mar. 2020, Art. no. 031005, doi: [10.1115/1.4045969](https://doi.org/10.1115/1.4045969).
- [2] C. M. Heyl, J. Gdde, A. Lhuillier, and U. Hfer, "High-order harmonic generation with J laser pulses at high repetition rates," *J. Phys. B: At., Mol. Opt. Phys.*, vol. 45, no. 7, Apr. 2012, Art. no. 074020, doi: [10.1088/0953-4075/45/7/074020](https://doi.org/10.1088/0953-4075/45/7/074020).
- [3] Z. Wei, S. Xu, Y. Jiang, Y. Gao, K. Zhao, and J. Zhu, "Principle and progress of attosecond pulse generation," *Chin. Sci. Bull.*, vol. 66, no. 8, pp. 889–901, Mar. 2021, doi: [10.1360/TB-2020-1525](https://doi.org/10.1360/TB-2020-1525).
- [4] K. Zhao *et al.*, "Principle and technology of attosecond pulse characterization," *Chin. Sci. Bull.*, vol. 66, no. 8, pp. 835–846, Mar. 2020, doi: [10.1360/TB-2020-1502](https://doi.org/10.1360/TB-2020-1502).
- [5] A. Tnnermann *et al.*, "100 W average power femtosecond laser at 343 nm," *Opt. Lett.*, vol. 41, no. 8, pp. 1885–1888, Apr. 2016, doi: [10.1364/OL.41.001885](https://doi.org/10.1364/OL.41.001885).
- [6] Y. Li *et al.*, "Diamond Raman laser: A promising high-beam-quality and low-thermal-effect laser," *High Power Laser Sci. Eng.*, vol. 9, 2021, Art. no. 35, doi: [10.1017/HPL.2021.25](https://doi.org/10.1017/HPL.2021.25).
- [7] C. Krnkel, G. Huber, and K. Petermann, "Solid-state lasers: Status and future," *J. Opt. Soc. Amer. B*, vol. 27, no. 11, pp. B93–B105, Nov. 2010, doi: [10.1364/JOSAB.27.000B93](https://doi.org/10.1364/JOSAB.27.000B93).
- [8] J. Chi *et al.*, "100-W 430-ps all-fiber picosecond laser by using 10-/130- $\mu\text{m}$  ytterbium-doped double-clad fiber and its application in SCS," *Appl. Phys. B: Lasers Opt.*, vol. 118, no. 3, pp. 369–377, Mar. 2015, doi: [10.1007/S00340-014-5993-9/FIGURES/12](https://doi.org/10.1007/S00340-014-5993-9/FIGURES/12).
- [9] D. Goular *et al.*, "Coherent beam combining of two femtosecond fiber chirped-pulse amplifiers," *Opt. Lett.*, vol. 36, no. 5, pp. 621–623, Mar. 2011, doi: [10.1364/OL.36.000621](https://doi.org/10.1364/OL.36.000621).
- [10] D. C. Brown, "The promise of cryogenic solid-state lasers," *IEEE J. Sel. Topics Quantum Electron.*, vol. 11, no. 3, pp. 587–599, May/Jun. 2005, doi: [10.1109/JSTQE.2003.850237](https://doi.org/10.1109/JSTQE.2003.850237).
- [11] L. E. Zapata, F. Reichert, M. Hemmer, and F. X. Krtner, "250 W average power, 100 kHz repetition rate cryogenic Yb:YAG amplifier for OPCPA pumping," *Opt. Lett.*, vol. 41, no. 3, Feb. 2016, Art. no. 492, doi: [10.1364/ol.41.000492](https://doi.org/10.1364/ol.41.000492).
- [12] T. Dietz, M. Jenne, D. Bauer, M. Scharun, D. Sutter, and A. Killi, "Ultrafast thin-pass amplifier system providing 1.9 kW of average output power and pulse energies in the 10 mJ range at 1 ps of pulse duration for glass-cleaving applications," *Opt. Exp.*, vol. 28, no. 8, Apr. 2020, Art. no. 11415, doi: [10.1364/oe.383926](https://doi.org/10.1364/oe.383926).
- [13] H. D. Hoffmann, J. Weitenberg, P. Russbldt, R. Poprawe, and T. Mans, "Compact diode-pumped 1.1 kW Yb:YAG innoslab femtosecond amplifier," *Opt. Lett.*, vol. 35, no. 24, pp. 4169–4171, Dec. 2010, doi: [10.1364/OL.35.004169](https://doi.org/10.1364/OL.35.004169).
- [14] D. Sangla *et al.*, "High power laser operation with crystal fibers," *Appl. Phys. B*, vol. 97, no. 2, pp. 263–273, Aug. 2009, doi: [10.1007/S00340-009-3666-X](https://doi.org/10.1007/S00340-009-3666-X).
- [15] X. Dlen *et al.*, "Single crystal fiber for laser sources," in *Proc. SPIE - Int. Soc. for Opt. Eng.*, Mar. 2015, Art. no. 934202, doi: [10.1117/12.2081184](https://doi.org/10.1117/12.2081184).
- [16] V. Markovic, A. Rohrbacher, P. Hofmann, W. Pallmann, S. Pierrot, and B. Resan, "160 W 800 fs Yb:YAG single crystal fiber amplifier without CPA," *Opt. Exp.*, vol. 23, no. 20, Oct. 2015, Art. no. 25883, doi: [10.1364/oe.23.025883](https://doi.org/10.1364/oe.23.025883).
- [17] F. Lesparre *et al.*, "Yb:YAG single-crystal fiber amplifiers for picosecond lasers using the divided pulse amplification technique," *Opt. Lett.*, vol. 41, no. 7, Apr. 2016, Art. no. 1628, doi: [10.1364/ol.41.001628](https://doi.org/10.1364/ol.41.001628).
- [18] N. N. Wang *et al.*, "23.9 W, 985 fs chirped pulse amplification system based on Yb:YAG rod amplifier," *IEEE Photon. J.*, vol. 11, no. 4, Aug. 2019, Art. no. 1503307, doi: [10.1109/JPHOT.2019.2926840](https://doi.org/10.1109/JPHOT.2019.2926840).
- [19] N. N. Wang *et al.*, "Development of a 67.8 W, 2.5 ps ultrafast chirped-pulse amplification system based on single-crystal fiber amplifiers," *Appl. Opt.*, vol. 59, no. 27, pp. 8106–8110, Sep. 2020, doi: [10.1364/AO.399680](https://doi.org/10.1364/AO.399680).
- [20] J. Yang *et al.*, "Femtosecond laser system based on thin rod active Yb:YAG elements with high average output power and pulse energy," *Quantum Electron.*, vol. 51, no. 10, pp. 873–877, Oct. 2021, doi: [10.1070/QEL17622/XML](https://doi.org/10.1070/QEL17622/XML).
- [21] A. M. Rodin and E. Zopelis, "Comparison of Yb:YAG single crystal fiber with larger aperture CPA pumped at 940 nm and 969 nm," in *Proc. Conf. Lasers Electro-Opt. Pacific Rim*, 2017, pp. 1–5, doi: [10.1109/CLEOPR.2017.8118912](https://doi.org/10.1109/CLEOPR.2017.8118912).

- [22] H. Chu, S. Zhao, and D. Li, "8.2  $\mu\text{J}$  5 PS Yb:KGW–Yb:YAG MOPA system at 1 MHz repetition rate," *Opt. Commun.*, vol. 450, pp. 176–179, Nov. 2019, doi: [10.1016/j.optcom.2019.05.059](https://doi.org/10.1016/j.optcom.2019.05.059).
- [23] L. Veselis, T. Bartulevicius, K. Madeikis, and A. Michailovas, "Generation of 40 W, 400 fs pulses at 1 MHz repetition rate from efficient, room temperature Yb:YAG double-pass amplifier seeded by fiber CPA system," in *Proc. SPIE 11259, Solid State Lasers XXIX: Technol. Devices*, 2020, Art. no. 1125925, doi: [10.1117/12.2545473](https://doi.org/10.1117/12.2545473).
- [24] X. Bu, Y. Xu, Z. Peng, H. Li, and P. Wang, "100 W, 7 PS hybrid Yb-fiber and Yb:YAG thin-rod MOPA laser," in *Proc. SPIE 11455, 6th Symp. Novel Optoelectron. Detection Technol. Appl.*, Apr. 2020, Art. no. 114553T, doi: [10.1117/12.2564717](https://doi.org/10.1117/12.2564717).
- [25] S. Chénais, F. Druon, S. Forget, F. Balembois, and P. Georges, "On thermal effects in solid-state lasers: The case of ytterbium-doped materials," *Prog. Quantum Electron.*, vol. 30, no. 4, pp. 89–153, Jan. 2006, doi: [10.1016/j.pquantelec.2006.12.001](https://doi.org/10.1016/j.pquantelec.2006.12.001).
- [26] S. M. Sohel Murshed and C. A. Nieto de Castro, "A critical review of traditional and emerging techniques and fluids for electronics cooling," *Renewable Sustain. Energy Rev.*, vol. 78, pp. 821–833, Oct. 2017, doi: [10.1016/j.rser.2017.04.112](https://doi.org/10.1016/j.rser.2017.04.112).
- [27] L. Gong, J. Zhao, and S. Huang, "Numerical study on layout of micro-channel heat sink for thermal management of electronic devices," *Appl. Thermal Eng.*, vol. 88, pp. 480–490, Sep. 2015, doi: [10.1016/j.applthermaleng.2014.09.048](https://doi.org/10.1016/j.applthermaleng.2014.09.048).
- [28] E. Anashkina and O. Antipov, "Electronic (population) lensing versus thermal lensing in Yb:YAG and Nd:YAG laser rods and disks," *J. Opt. Soc. Amer. B*, vol. 27, no. 3, pp. 363–369, Mar. 2010, doi: [10.1364/JOSAB.27.000363](https://doi.org/10.1364/JOSAB.27.000363).
- [29] I. I. Kuznetsov, S. A. Chizhov, I. B. Mukhin, and O. V. Palashov, "Technology of thin-rod Yb:YAG amplifiers with a high pulse energy and average power," *Quantum Electron.*, vol. 50, no. 4, pp. 327–330, Apr. 2020, doi: [10.1070/QEL17279/XML](https://doi.org/10.1070/QEL17279/XML).
- [30] X. Yan, P. Zhigang, S. Yuhang, W. Beibei, C. Zhaochen, and W. Pu, "Hundred-watt-level 1030 nm fiber-bulk hybrid amplified laser," *J. Infrared Laser Eng.*, vol. 502, 2022, Art. no. 127428, doi: [10.3788/IRLA20210442](https://doi.org/10.3788/IRLA20210442).
- [31] A. Ikesue *et al.*, "Thermal-birefringence-induced depolarization in Nd:YAG ceramics," *Opt. Lett.*, vol. 27, no. 4, pp. 234–236, Feb. 2002, doi: [10.1364/OL.27.000234](https://doi.org/10.1364/OL.27.000234).
- [32] X. Y. Jiang, X. W. Yan, Z. G. Wang, J. G. Zheng, M. Z. Li, and J. Q. Su, "Influence of thermal reduced depolarization on a repetition-frequency laser amplifier and compensation," *High Power Laser Sci. Eng.*, vol. 3, 2015, Art. no. 9, doi: [10.1017/HPL.2015.4](https://doi.org/10.1017/HPL.2015.4).
- [33] H. Nishioka *et al.*, "High-energy, diode-pumped, picosecond Yb:YAG chirped-pulse regenerative amplifier for pumping optical parametric chirped-pulse amplification," *Opt. Lett.*, vol. 32, no. 13, pp. 1899–1901, Jul. 2007, doi: [10.1364/OL.32.001899](https://doi.org/10.1364/OL.32.001899).